Summary and Conclusions

An analytical solution has been obtained for the displacement and rotation angle of a single-joint flexible robot modeled by a continuous, clamped-free beam attached to a rigid hub of negligible radius. The results for a representative-applied harmonic torque are obtained and show the effect of the beam flexibility, which can be superimposed on the rigid-beam motion. Fourier series representations can be applied in the usual way to generalize these results. The nondimensionalization for both dynamic equations permitted a simpler problem formulation. The solution also provides a quick means of testing the effect of the various physical parameters on the design of a flexible one-link robot. The solution gives the accurate location of every point of the link and, thus, changing the parameters can give the desired results for a specific task for the arm.

Acknowledgments

This material is based on work supported by the National Science Foundation under Contract 0814285. The authors would like to thank Kurt Moesslacher and Peter Stokes for performing the numerical computations leading to the results presented herein.

References

[1]Kane, T. R., Ryan, R. R., and Banerjee, A. K., "Dynamics of a Cantilever Beam Attached to a Moving Base," *Journal of Guidance, Control, and Dynamics,* Vol. 10, March–April 1987, pp. 139–151.

[2]Cannon, R. H., Jr., and Schmitz, E., "Initial Experiments on the End-Point Control of a Flexible One-Link Robot," *International Journal of Robotics Research,* Vol. 3, No. 3, Fall 1984, pp. 62–75.

[3]Chassiakos, A. G. and Bekey, G. A., "Pointwise Control a Flexible Manipulator Arm," *Proceedings of the Symposium of Robot Control,* Nov. 1985, pp. 113–117.

[4]Hastings, G. G. and Book, W. J., "Experiments in the Control of a Flexible Robot Arm," *Conference Proceedings Robots 9, Robotics International Journal of Society of Manufacturing Engineering,* Vol. 2, June 1985, pp. 20-45 to 20-57.

[5]Rakhsha, F. and Goldenberg, A. A., "Dynamics Modeling of a Single-Link Flexible Robot," *Proceedings of the IEEE International Conference on Robotics and Automation,* IEEE, New York, March 1985, pp. 984–989.

[6]Sakawa, Y., Matsuno, F., and Fukushima, S., "Modeling and Feedback Control of a Flexible Arm," *Journal of Robotic Systems,* Vol. 2, No. 4, Winter 1985, pp. 453–472.

[7]Wie, B. and Bryson, A. E., "Pole-Zero Modeling of Flexible Space Structures," *Journal of Guidance, Control, and Dynamics,* (to be published).

Enhancement of Data Separability in Multisensor-Multitarget Tracking Problems

S. N. Balakrishnan*
University of Missouri—Rolla, Rolla, Missouri
and
B. D. Tapley† and B. E. Schutz‡
University of Texas at Austin, Austin, Texas

Introduction

IN many current tracking problems, the tracking scenario may involve multiple targets whose states are to be estimated with observations from several sensors. The various aspects of the multitarget problems and the outlines of different solution techniques are given in Ref. 1.

In this Note, improvements to a clustering analysis-based modular approach[2] are made through the use of observation residuals. In such an approach, the multitarget problem is reduced to several single-target problems.

Simulation Models

The mathematical models of motion of the targets and the observations are presented here. The target motion is confined to two dimensions only. The scenarios considered here consist of moving targets and stationary observers.

System Model

The state vector consists of the reference Doppler frequency, f_0, the position components, x and y, velocity components, $\dot{x}$ and $\dot{y}$, and the acceleration components, a_x and a_y, of the target in an inertial x-y coordinate frame. The state vector is given by

$$X = [f_0, x, y, \dot{x}, \dot{y}, a_x, a_y]^T \tag{1}$$

The Doppler frequency and the target acceleration are modeled as constants driven by white noise processes. Consequently, the differential equation of motion of the target is

$$\dot{X} = AX + W \tag{2}$$

where

$$A = \begin{bmatrix} 0_{7\times 3} & \vdots & \begin{matrix} 0_{1\times 4} \\ I_{4\times 4} \end{matrix} \\ & \vdots & 0_{2\times 4} \end{bmatrix} \tag{3}$$

and

$$W = [w_f, 0, 0, 0, 0, w_x, w_y]^T \tag{4}$$

w_f, w_x, and w_y are assumed to be zero-mean white Gaussian processes with power spectral densities of q_f, q_x, and q_y, respectively.

Measurement Model

In this study, the three components of the measurement vector, y, are the Doppler frequency, f, the sine of the bearing angle, and the cosine of the bearing angle measured between the signal source/sensor line and the reference x direction.[3]

The relation between the frequency shift and the relative speed of a signal source moving with respect to the sensor is

$$y_1 = f = \frac{f_0}{1 + v_R/c} \tag{5}$$

where f is the received frequency, f_0 the transmitted frequency, v_R the relative velocity of the source with respect to the sensor, and c the speed of sound in the propagated medium. The relative velocity, v_R, is given by $v_R = [(x - x_s)\dot{x} + (y - y_s)\dot{y}]/R$, where x_s and y_s are the sensor coordinates in the inertial x-y coordinates and $R = [(x - x_s)^2 + (y - y_s)^2]^{\frac{1}{2}}$. The bearing angle θ is defined as the angle between the x axis and the line joining the sensor and the target. The other two measurements are

$$y_2 = \sin\theta = (y - y_s)/R \tag{6}$$

and

$$y_3 = \cos\theta = (x - x_s)/R \tag{7}$$

Received Dec. 1, 1987; revision received July 6, 1988.

*Assistant Professor. Senior Member AIAA.
†Professor. Fellow AIAA.
‡Professor. Associate Fellow AIAA.

Numerical Results

In order to demonstrate the enhanced data separability by using the residuals in the modular approach, two different scenarios involving two maneuvering targets are considered. The two-dimensional trajectory for each target is the same for each scenario; however, the sensor distances from the targets are varied. The idea is to decrease the signal-to-noise ratio in the second case by increasing the distance of the targets from the sensors. Five sensors are used to collect the observations. The target trajectories and the sensor locations are presented in Fig. 2. The collection of simulated data using the models described in the preceding section corresponds to step 1 in Fig. 1.

The 101 measurements are collected at 10-s intervals over 1000 s. The measurement standard deviations are 0.1 Hz for the frequency and 5 deg for the bearing angle. The data thus collected from each sensor are merged to form a multitarget data set as in step 2 of Fig. 1 and used as input to the single-linkage hierarchical technique[4] as shown in step 3 of Fig. 1.

Clustering techniques seek to sort data points into natural groups based on their attributes. The attributes of a sample point here are the normalized values (between 0 and 1) of the *time* and the meaurements. The metric to group the data points is the average Euclidean distance between a pair of points.[2] The application of the clustering technique to the data collected by each sensor from scenario 1 shows two distinct clusters (represented by significant jumps in the tree diagram, an output from the clustering technique). Each cluster is found (manually) to consist of all the 101 correct data for the different targets. As an example outcome of this sorting process, the combined frequency data from sensor 1 observing this scenario are given in Fig. 3. From the tree diagram, the frequency data corresponding to target 1 are identified from one cluster of data and presented in Fig. 4. Similarly, the data corresponding to target 2 are gathered from the second cluster of the tree diagram and presented in Fig. 5. In order to merge the data from different sensors corresponding to each target, the batch filtering process[5] is used on pairs of data clusters from different sensors, as indicated by step 4 in Fig. 1. Convergence of the batch process on initial conditions of the state indicates proper data correlation. Improper fusion of data pairs leads to divergence of the initial state. Note that the process noise variances are not included in the batch filter in order to avoid increasing the

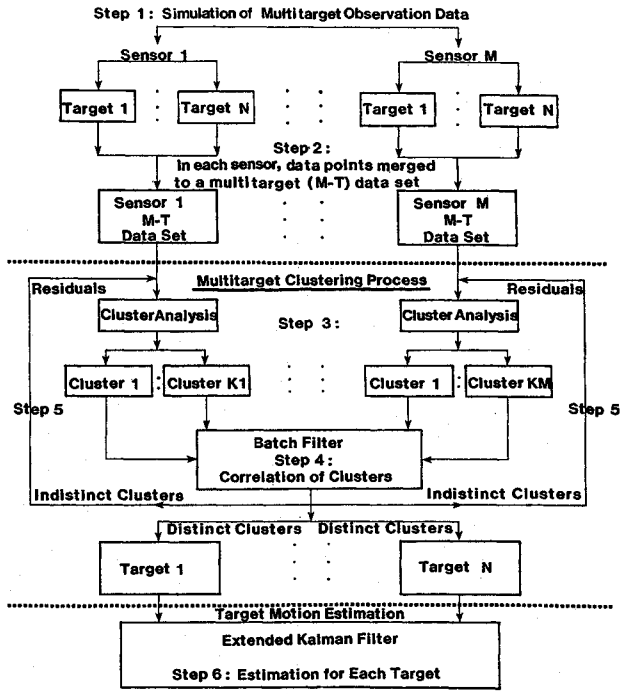

Fig. 1 Diagram for data flow.

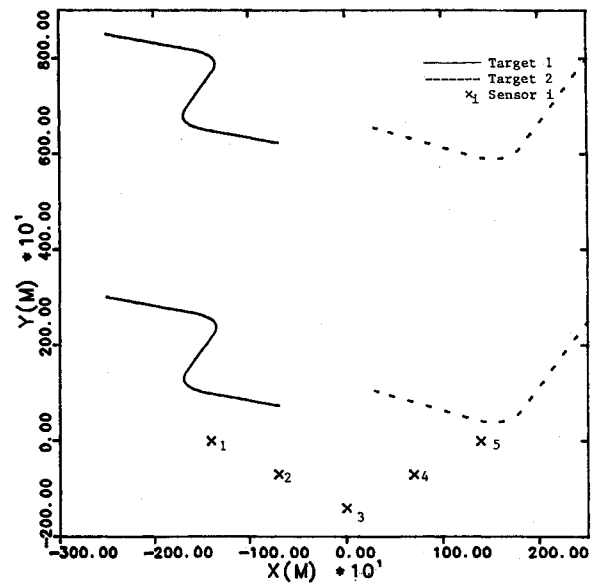

Fig. 2 Trajectories of targets and locations of sensors.

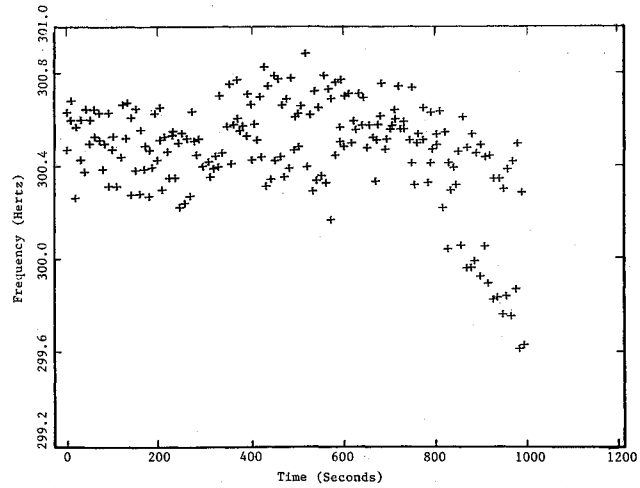

Fig. 3 Frequency measurements from sensor 1, scenario 1.

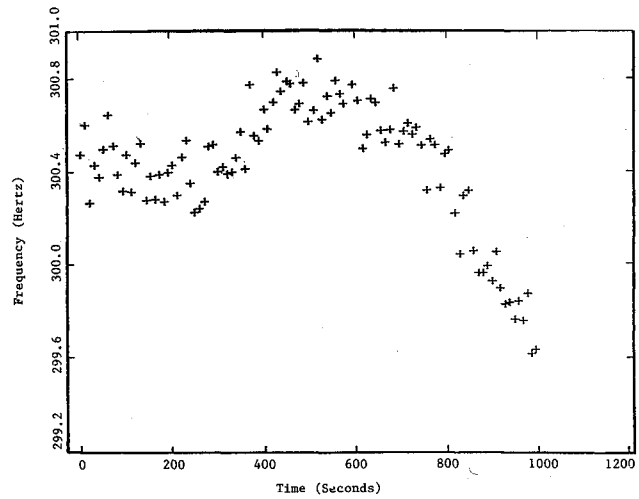

Fig. 4 Cluster result of frequency from sensor 1 for target 1 in scenario 1.

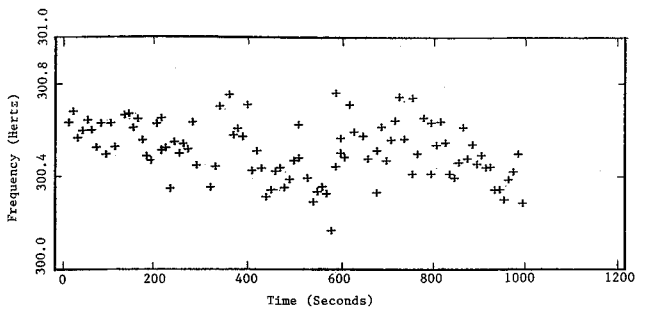

Fig. 5 Cluster result of frequency from sensor 1 for target 2 in scenario 1.

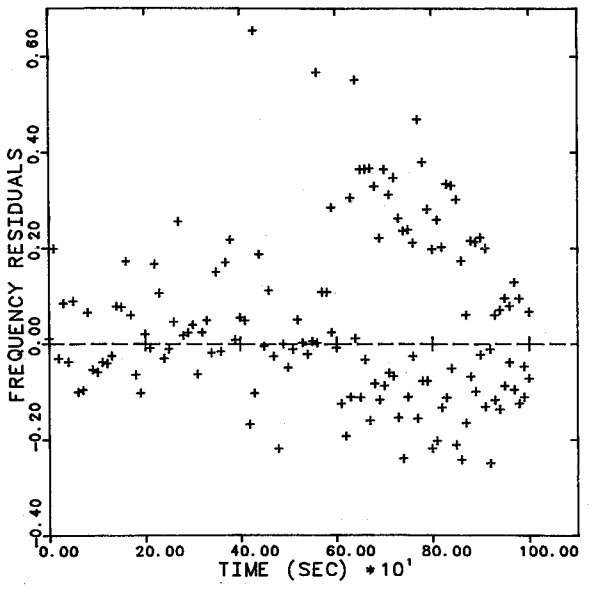

Fig. 6 Doppler frequency residuals of target 1 and unassigned points from sensor 2.

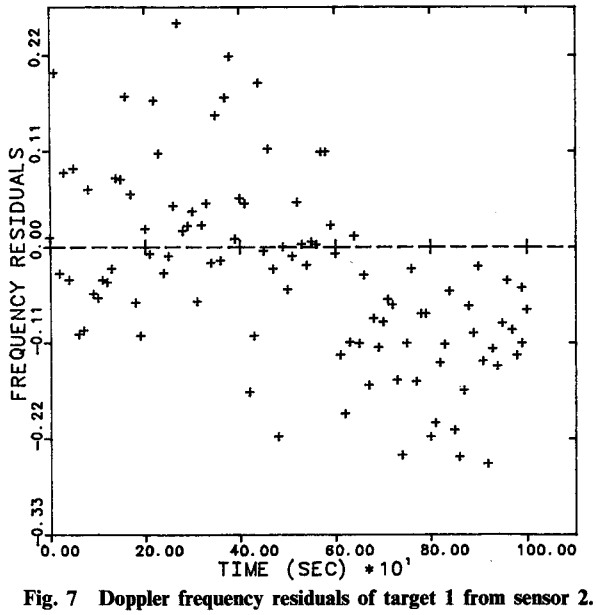

Fig. 7 Doppler frequency residuals of target 1 from sensor 2.

high computational load associated with the batch process. By successive application of the batch filter, the data clusters corresponding to each target from different sensors are merged pairwise and, with the initial conditions obtained from the batch process, the extended Kalman filter[5] is used to obtain the trajectories of *each* of the targets with the data from all five sensors. This corresponds to step 6 in Fig. 1. The initial condition for the filter is the estimated state from the batch process. The diagonal elements of the initial state covariance are 10^7 and of the process noise covariance are 10^{-6} corresponding to the frequency and accelerations. All other elements are set at zero.

When the raw data from a set of distant targets from scenario 2 are input to the clustering technique, however, the sorting is not as good and there are three distinct groups of data appearing in the tree diagram results for sensors 2 and 4. Sensor 1 has 100, 60, and 40 data in three clusters and sensor 4 has clusters with 98, 66, and 35 data. The reason for this phenomenon lies in the fact that the targets are far from the sensors even though their motions are the same as in scenario 1. The longer distances reduce the distinction in the bearing measurements. This factor causes more difficulty for the clustering process to discriminate the data. Clustering of the data from sensors 2, 3, and 5 shows two distinct clusters of data with 100 and 98 data, 99 and 97 data, and 98 and 101 data, respectively. The higher number of points in each cluster are found to belong to target 1 with the use of batch processing. Similarly, the two dominant clusters with 60 data points from sensor 1 and 66 data points from sensor 4 are found to be associated with target 2 along with the other sensor data, again through the batch filter. In order to examine and utilize more data, *observation residuals* of all the data for target 1 and the unassigned points (40 from sensor 1, and 35 from sensor 4) are obtained by making a pass through the batch algorithm with the initial conditions from the converged results of target 1. The residuals for each sensor are then processed through the clustering procedure as indicated by step 5 in Fig. 1. The Doppler frequency residuals of all the points from sensor 1 and the sorted residuals corresponding to target 1 from sensor 1 are presented in Figs. 6 and 7, respectively. Similar separation is also noticed with data from sensor 4. When the residuals are obtained by using target 2 dynamics, data and unassigned points are generated, the tree diagram shows only one distinct cluster for each sensor. The sorted data points through the use of residuals are 101 and 100, 100 and 101, 100 and 101, 101 and 101, 98 and 101 for sensors 1 through 5, respectively. Note that, finally, only 6 points out of 1010 could not be identified clearly. Spurious data also can be similarly rejected. In the process of using the residuals, if distinct clusters (more than 2) had still persisted, they should have been interpreted as a third (or new) target.

With the initial state estimate from the batch filter as in the first scenario, an extended Kalman filter is used to estimate the states of the individual targets.

Conclusions

An extension to the use of a modular approach to the multisensor/multitarget problem has been presented. The validity of the use of the observation residuals in the data discrimination process and the data-target correlation has been demonstrated through application of the algorithm in a simulated underwater tracking problem.

References

[1]Bar-Shalom, Y., "Tracking Methods in Multitarget Environment," *IEEE Transactions on Automatic Control*, Vol. AC-23, Aug. 1978, pp. 618–626,

[2]Balakrishnan, S. N. and Tapley, B. D., "Application of Clustering Techniques for the Detection, Classification, and Estimation of Multiple Targets in Space," AIAA Paper 88-0571, Jan. 1988.

[3]Tapley, B. D., Schutz, B. E., Ho, C. S., and Wilson, T., "Data Classification for Multitarget Tracking Applications," Center for Space Research, The Univ. of Texas at Austin, CSR-83-5, May 1983.

[4]Andenberg, M. R., *Cluster Analysis for Applications*, Academic, New York, 1973.

[5]Jazwinski, A., *Stochastic Processes and Filtering Theory*, Academic, New York, 1970.